

Quantum Conductance of Achiral Graphene Ribbons and Carbon Nanotubes

Lyuba Malysheva¹ and Alexander Onipko^{1,*}

¹*Bogolyubov Institute for Theoretical Physics, 03680 Kyiv, Ukraine*

(Dated: January 8, 2019)

Explicit expressions of the band spectrum near the neutrality point for armchair and zigzag graphene ribbons and carbon nanotubes were derived based on a tight-binding macromolecule model of graphene. The obtained dispersion relations are used to determine and compare the conductance ladders of these structures and are beneficial for many other applications. Our results are different in many respects from previously reported data. This new information forms a solid reliable basis for evaluation of the potential of graphene nanoelectronic devices.

INTRODUCTION

Conductance quantization, discovered in split-gate configurations of two-dimensional electron gas (2DEG) [1, 2], is a classic quantum phenomena that can be easily understood on the basis of the Landauer formula [3, 4]

$$G = G_0 \sum_j g_j T_j(E_F) = G_0 T(E_F). \quad (1)$$

The formula identifies the zero-bias, zero-temperature conductance G , in units of conductance quantum $G_0 = 2e^2/h$, with the transmission coefficient $T(E_F)$. In Eq. (1), the sum runs over all propagating modes j with energies below the Fermi energy E_F , factor g_j accounts for the mode (or corresponding 1D band) degeneracy. The conductor is supposed to be free of defects, so that the mode-to-mode transmission is absent, $T_{jj'}(E_F) = \delta_{jj'} T_j(E_F)$. In the absence of scattering, all we need to know is the opening energies (e.g., band bottoms) of propagating states and their degeneracy. As a function of E_F , the conductance of 2DEG narrow channels assumes a form, well resembling a ladder (*conductance ladder*) of equidistant steps with equal height G_0 [5]. The role of different factors, which affect the shape of the ladder steps has been studied in detail [6, 7, 8].

Graphene structures, such as graphene ribbons and carbon nanotubes, suggest 1D wires made of one-atom thick material that offer a natural 2D media for current carriers, electrons and holes. After the discovery of graphene and the elucidation of its unique electronic properties [9], graphene-based electronics has received intriguing scientific and practical attention. The conductance ladder in graphene structures is expected to have a different appearance than its 2DEG counterparts. Therefore, a clear theoretical model of quantum conductance with direct references to the graphene atomic and electronic structures is important. Our work and this report gives a precise description of the conductance of four basic graphene wires and specific features of each member of the wire family.

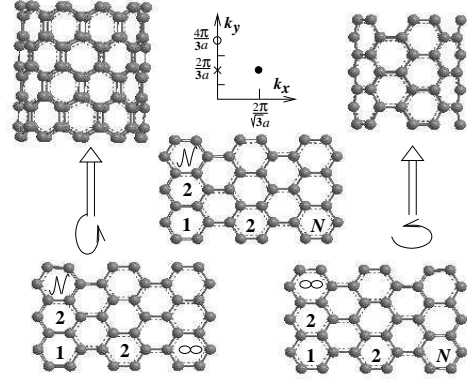


FIG. 1: Parent graphene $N \times N$ lattice (center) and its daughter structures, from lower-left and on clockwise: armchair ribbon ($N = \infty$); $(N, 0)$ nanotube ($N = \infty$, 1-st = $N + 1$ -th polyacene chain); (N, N) nanotube ($N = \infty$, 1-st = $N + 1$ -th polyparaphenylene chain); and zigzag ribbon ($N = \infty$). In all cases, same k -coordinates are used. Cross $(0, \frac{2\pi}{3a})$ and circle $(0, \frac{4\pi}{3a})$ indicate zero-energy points: x for armchair GRs, x and o for zigzag metallic CNTs; filled circle $(\frac{2\pi}{\sqrt{3}a}, \frac{2\pi}{3a})$ indicates the second special point for armchair CNTs. For zigzag GRs, zero-energy point cannot be shown on real k_x - k_y plane, see text.

METHODOLOGY AND RESULTS

Figure 1 illustrates the parent honeycomb $N \times N$ lattice, in the center, and its daughter wire-like structures, armchair and zigzag graphene ribbons (GRs) and carbon nanotubes (CNTs). The lattice label indicates that in the armchair direction, graphene contains N hexagons in polyparaphenylene-like chains, whereas in the zigzag direction, it has N hexagons, forming polyacene-like chains. This is the structure of a plane, all-carbon macromolecule, terminated by hydrogens along armchair and zigzag edges. For the canonical tight-binding Hamiltonian of such macromolecule, the exact dispersion relation

reads [10]

$$E^\pm = \pm \sqrt{1 + 4 \cos^2 \frac{ak_y}{2} \pm 4 \left| \cos \frac{ak_y}{2} \cos \frac{\sqrt{3}ak_x}{2} \right|}, \quad (2)$$

where the hopping integral t is used as an energy unit, a is the minimal translation distance of honeycomb lattice, and the range of variation of k_x and k_y corresponds to the full basis set that was used for the derivation of Eq. (2). This range should be specified for each particular type of the wires.

Distinct from the zone folding technique [11, 12], which requires a certain projection of the 2D graphite band structure on the zigzag or armchair direction, we avoid this extra complication by using the same k -coordinates for all the wires in focus. Differences in the formal description of these wires come from the two factors: (i) which of two dimensions N or \mathcal{N} is infinite, that is prescribing continuity to k_x or k_y for, respectively, armchair GRs and zigzag CNTs or zigzag GRs and armchair CNTs; and (ii) which boundary conditions, the open ends for GRs or periodic for CNTs, are used to determine the complementary discrete quantum number, k_y or k_x . Thus, for graphene ribbons, the k space is $(0-\pi, 0-\pi)$; for armchair and zigzag carbon nanotubes, the required extensions of this space are, respectively, $(0-2\pi, 0-\pi)$ and $(0-\pi, 0-2\pi)$. Because of these extensions, the degeneracy of electron states increases as discussed below. Finally, for the models at hand, the spectra of armchair GRs and both types of CNTs are completely determined by Eq. (2), complemented by corresponding values of the discrete quantum number. An additional equation, Eq. (8), comes into play in the discussion of zigzag GRs.

We shall consider pairs of related GR and CNT structures separately. The focus is on the energies that are not far away from the point of neutrality; here, it is $E_F = 0$. In this energy region, the spectrum is described by the minus branch of Eq. (2) (minus sign under the root). This part of the spectrum will be rationalized in terms of two quantum numbers, longitudinal (continuous) and transverse (discrete). Because of the spectrum symmetry, we will refer only to the conduction 1D bands, that is to E^- branch with sign plus in front of the root. The valence bands, having the same transverse quantum numbers, are just a mirror reflection of the conduction bands in $E = 0$ plane. Most of the analysis refers (if not stated otherwise) to large N and \mathcal{N} . This simplification could be easily avoided, but even for $N, \mathcal{N} > 10$, it is sufficiently good for reasonable estimates.

Conductance of Armchair Ribbons and Zigzag Nanotubes

For both structures, armchair GRs and zigzag CNTs, k_x is a continuous variable $0 \leq \sqrt{3}ak_x \leq \pi$. Whereas the

wave vector transverse component takes discrete values $k_y = \xi_j/a$, $\xi_j = \pi j/(\mathcal{N} + 1)$ and $\xi_j = 2\pi j/\mathcal{N}$, $j = 1, 2, \dots, \mathcal{N}$ for ribbons and nanotubes, respectively. An immediate consequence of this difference in quantization is that 1D bands in zigzag CNTs are twofold degenerate, whereas they are not degenerate in armchair GRs.

It is well known that armchair (zigzag) GRs (CNTs) are metallic if $j^* = 2(\mathcal{N} + 1)/3$ ($j^* = \mathcal{N}/3$) is an integer. In such a case, $E_{j^*}^-(k_x=0) = 0$; otherwise, these wires are semiconducting. Twofold band degeneracy of electron states in metallic zigzag CNTs is due to the fact that there are two zero-energy points, $(0, \xi_{j^*})$ and $(0, 2\xi_{j^*})$; or, equivalently, $(k_x = 0, ak_y = 2\pi/3)$ and $(k_x = 0, ak_y = 4\pi/3)$, represented by cross and open circle in Fig. 1. For semiconducting armchair GRs (zigzag CNTs) the lowest conduction/highest valence mode j^* can be equal to $(2\mathcal{N} + 1)/3$ or $(2\mathcal{N} + 3)/3$ [$(\mathcal{N} - 1)/3$ or $(\mathcal{N} + 1)/3$].

The next conclusion that follows from the analysis of Eq. (2) is that the band spectrum of metallic graphene ribbons (carbon nanotubes) has a fine structure. This implies that the band bottoms, $E_{j^* \pm \mu}^-(k_x=0) \equiv E_{j^* \pm \mu}^-$, $\mu = 0, 1, \dots$, which correspond to μ and $-\mu$, have different energies,

$$E_{j^* \pm \mu}^- = \mu \Delta_{\text{GR(CNT)}}^{a(z)} \left(1 \pm \frac{1}{6} \mu \Delta_{\text{GR(CNT)}}^{a(z)} \right), \quad (3)$$

where $\Delta_{\text{CNT}}^z = 2\Delta_{\text{GR}}^a = \sqrt{3}\pi/\mathcal{N}$, and $\mu \ll \mathcal{N}$. Thus, the band spectrum of metallic armchair GRs and zigzag CNTs appears as a sequence of (approximately) equidistant pairs of close bands. The spacing between the lower bands in these pairs is constant and $\sim 1/\mathcal{N}$, but the band separation within pairs is $\sim 1/\mathcal{N}^2$ and increases $\sim \mu^2$. Consequently, the conductance ladder contains a sequence of long/short steps, see inset in Fig. 2. However, the close pairs of bands might not be resolved, as illustrated in Fig. 2; in other words, the fine structure may manifest itself as an apparent level degeneracy. Then, the apparent conductance quantization will be two times larger, than expected, $2G_0$ for armchair GRs, and $4G_0$ for zigzag CNTs.

The band spectrum near zero-energy points can be obtained by exploiting the condition $\mu \ll \mathcal{N}$ and $ak_x \ll 1$ in Eq. (2). As a result, we arrive at

$$\frac{E_{j^* \pm \mu}^-}{\Delta_{\text{GR(CNT)}}^{a(z)}} = \begin{cases} \sqrt{\mu^2 (1 \pm \frac{1}{6} \mu \Delta_{\text{GR(CNT)}}^{a(z)})^2 + X^2}, \\ \sqrt{(\pm \mu - \frac{1}{3})^2 + X^2}, \end{cases} \quad (4)$$

where the upper and lower lines refer to metallic and semiconducting GRs (CNTs), respectively, and a new notation, $X = \frac{\sqrt{3}}{2}ak_x/\Delta_{\text{GR(CNT)}}^{a(z)}$, is introduced. The validity of these dispersion relations is ensured by the condition $\mathcal{N}ak_x \ll \mu \neq 0$. Disregarding the fine structure in Eq. (4), one comes to the earlier suggested expression of

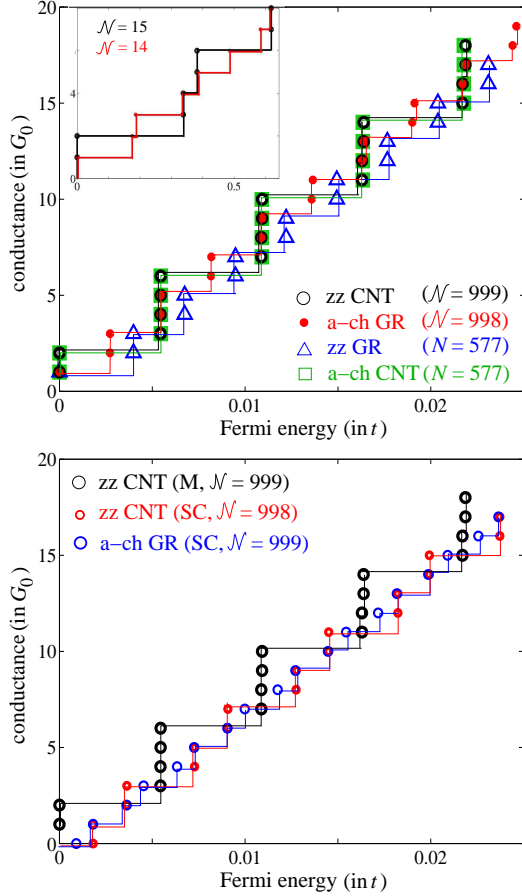


FIG. 2: Conductance ladders of different metallic (M) and semiconducting (SC) graphene-based wires. The ladders are slightly off-set for clarity. Markers indicate band opening. Fine band structure is well seen in conductance ladders of metallic zigzag CNTs (armchair GRs) with diameter (width) ~ 5 nm or smaller, as illustrated in inset. For about 250 nm wide graphene ribbons and same circumference length of rolled graphene, splitting of lower steps of black and red ladders is not resolved; splitting of higher steps into pairs of short/wide steps discloses the fine band structure, that is the removal of band apparent degeneracy.

the band spectrum for $(\mathcal{N}, 0)$ CNTs [13]. The latter gives an oversimplified description of conducting properties of zigzag metallic carbon nanotubes, see an inset in Fig. 2.

The obtained expressions for the band spectrum of armchair graphene ribbons and zigzag carbon nanotubes can easily be translated into the conductance ladders shown in Fig. 2. For these nanotubes, both the step height and width is two times larger, than for respective ribbons; specifically, change in the conductance $2G_0$ versus G_0 under the change in the Fermi energy $2\Delta_{\text{GR}}^a$ versus Δ_{GR}^a . Thus, the slope of the corresponding conductance ladders is the same, implying the equivalence of carbon nanotubes and graphene ribbons as classic conductors. Their difference as quantum wires is impressive and can be observed under appropriate experimental conditions.

Conductance of Armchair Nanotubes and Zigzag Ribbons

Conductance of these two types of graphene wires has to be considered separately, because unlike armchair GRs and zigzag CNTs, their formal description cannot be unified.

Case of Armchair Nanotubes

Now it is $ak_x = \kappa_\nu/\sqrt{3}$ that plays the role of transverse quantum number, $\kappa_\nu = 2\pi\nu/N$, $\nu = 0, 1, \dots, N-1$, whereas $0 \leq ak_y \leq \pi$ is a continuous variable [10]. Equation (2) can thus be rewritten as

$$E_\nu^\pm = \sqrt{1 + 4 \cos^2(ak_y/2) \pm 4 |\cos(ak_y/2) \cos(\pi\nu/N)|}. \quad (5)$$

As seen, all ν bands, with an exception of $\nu=0$ band, are twofold degenerate. Close to zero energy, that is for $|q| \ll 1$, $q = ak_y - 2\pi/3$, and $\pi\nu/N \ll 1$ or $\pi(N-\nu)/N \ll 1$ Eq. (5) is well approximated by

$$E_\nu^-(q) = \frac{1}{2} \sqrt{3q^2 + (2\Delta_{\text{CNT}}^a \nu)^2 (1 - \sqrt{3}q/2)}, \quad (6)$$

showing that the spectrum consists of a set of pseudo-parabolic bands with the bottoms at $q = q_\nu^a = \frac{\pi^2 \nu^2}{\sqrt{3}N^2}$,

$$E_\nu^{b-} = \nu \Delta_{\text{CNT}}^a \left[1 - \frac{1}{8} (\nu^2 \Delta_{\text{CNT}}^a)^2 \right], \quad \nu \Delta_{\text{CNT}}^a \ll 1, \quad (7)$$

where $\Delta_{\text{CNT}}^a = \pi/N$. The latter quantity would be the band spacing, if the linear term under the root (6) were disregarded, as it was done in Ref. [13]. Also worth noting is that for $\mathcal{N} = \sqrt{3}N$, $\Delta_{\text{CNT}}^a = \Delta_{\text{CNT}}^z = 2\Delta_{\text{GR}}^a$. Hence, the spectrum of armchair CNTs contains a nondegenerate band $\nu=0$, having linear dispersion, followed by a manifold of degenerate ν and $N-\nu$ bands with pseudo-parabolic dispersion. This is similar to the case of metallic zigzag CNTs. However, an important distinction is that in armchair CNTs, there are two propagating states which have different wave vectors, $q < q_\nu^a$ and $q > q_\nu^a$ (the smaller value of q is negative but both values of k_y are positive) which correspond to the same energy. So, the first step of the conductance ladder has $2G_0$ height and E_1^{b-} width, after which follows a manifold of $4G_0$ -high steps with slowly decreasing spacing between successive steps, $E_{\nu+1}^{b-} - E_\nu^{b-} = \Delta_{\text{CNT}}^a \{1 - (\Delta_{\text{CNT}}^a)^2 [3\nu(\nu+1) + 1]/8\}$.

The conductance ladders of armchair and zigzag CNTs are compared in Fig. 2. The most important distinction is that there is no fine structure in (N, N) CNT ladders whereas it is very prominent in metallic $(\mathcal{N}, 0)$ CNTs of a small diameter.

Case of Zigzag Ribbons

A cut of armchair CNT along zigzag direction and "healing" damages of three-coordinated sp^2 bonding by hydrogens, gives a zigzag graphene ribbon. Distinct from the types of graphene wires where the transverse quantum numbers were determined by open ends for armchair GRs and by periodic boundary conditions for $(N, 0)$ and (N, N) CNTs, for zigzag GRs discrete values of $0 < ak_x = \kappa_\nu^\pm / \sqrt{3} < \pi$ are k_y -dependent. These values can be found by solving

$$\frac{\sin \kappa^\pm N}{\sin \kappa^\pm (N + 1/2)} = \mp 2 \cos(ak_y/2), \quad (8)$$

where minus (plus) sign of the right hand side of this equation corresponds to plus (minus) branch of dispersion relation (2) [14]. Combining Eq. (2) and Eq. (8), one obtains

$$E^\pm = \mp \frac{\sin(\kappa^\pm/2)}{\sin \kappa^\pm (N + 1/2)}. \quad (9)$$

Extrema of E^- as a function of κ^- are given by solutions to equation

$$\frac{\sin(\kappa^- N)}{\sin \kappa^- (N + 1)} = \frac{N}{N + 1}. \quad (10)$$

This simplifies finding minima (maxima) of conduction (valence) bands as functions of k_y . Equations (8)–(10) are exact; to obtain an explicit expression of the band structure, certain approximations have to be made.

For any value of k_y , the minus branch of Eq. (8) has N solutions one of which is imaginary, $\kappa_0^- = i\delta$, if k_y falls into the interval $2\pi/3 + (\sqrt{3}N)^{-1} < ak_y \leq \pi$. In the latter case and under the restriction $\delta N \gg 1$, it follows from Eqs. (8) and (9) that

$$E^- = \frac{\sinh(-\ln[2\sin(\pi/6 - q/2)])}{\sinh(-\ln[2\sin(\pi/6 - q/2)](2N + 1))}. \quad (11)$$

This equation describes a part of the lowest conduction band (dispersion of edge states) [14]. The other part of the band is similar to that which has $\nu=0$ band of armchair CNTs, see Fig. 3. To obtain an analytical expression for this part and dispersion in higher lying bands, one has to find real solutions to Eq. (10), $\kappa_\nu^- \approx (\nu + 1/2)\pi/N$, $\nu = 0, 1, \dots, \nu \ll N$, and use them in Eq. (2). This gives

$$E_\nu^-(q) = \frac{1}{2} \sqrt{3q^2 + [(2\nu + 1)\Delta_{\text{GR}}^z]^2 \left(1 - \sqrt{3}q/2\right)}, \quad (12)$$

which for $\nu = 0$ and $q > 0$ should be replaced by Eq. (11). Bottoms of $\nu > 0$ bands are determined by

$$E_\nu^{b-} = (\nu + 1/2)\Delta_{\text{GR}}^z \left(1 - \frac{1}{8}[(\nu + 1/2)\Delta_{\text{GR}}^z]^2\right), \quad (13)$$

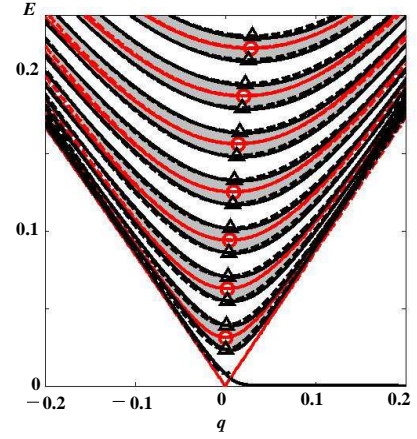


FIG. 3: 1D bands $\nu = 0, 1, \dots, 7$ of (N, N) CNT (in red) and $\nu = 0, 1, \dots, 14$ of N -wide zigzag GR, $N = 100$ (black lines). Exact calculations are represented by solid lines. These pair off with their (often indistinguishable) approximations indicated by dashed lines. Linear dispersion and all curves in the mid of shaded areas dispose the CNT band structure, explicitly expressed in Eq. (6). Rest of the curves corresponds to zigzag GR, approximated by Eqs. (11) and (12). The band minima calculated according Eqs. (7) and (13) are shown by circles and triangles, respectively.

these energies are attained at $q \equiv q_\nu^z = \frac{\pi^2(\nu+1/2)^2}{4\sqrt{3}N^2}$, $\nu = 1, 2, \dots$. Notice, the interband separation in zigzag GRs is well approximated by $\Delta_{\text{GR}}^z = \Delta_{\text{CNT}}^a/2 = \pi(2N)^{-1}$. This ratio between Δ_{GR}^z and Δ_{CNT}^a is exactly the same as for pairs zigzag CNTs–armchair GRs.

So, in contrast to armchair CNTs, the dispersion of the lowest conduction band of a zigzag GR is a decreasing function of the wave vector. In Fig. 3, it is represented by the lowest black line. An almost linear decrease for $ak_y \leq 2\pi/3$ changes (within the interval $(2\pi/3, 2\pi/3 + (\sqrt{3}N)^{-1})$ to an exponential-like (11) that governs dispersion up to the maximal value of $ak_y = \pi$, see [14] for details. The rest of the band structure of zigzag GRs near the neutrality point, as illustrated in Fig. 3, is very similar to the one we obtained for armchair CNTs. However, obtaining Eq. (12) is far from being equally straightforward.

A visual comparison of approximations (6) and (11)–(12) (dashed lines in Fig. 3) with exact calculations (solid lines in Fig. 3) proves both approximations as very accurate. Explicit expressions of the band structures and the knowledge of their degeneracy makes obvious the interrelation between the conductance ladders of achiral GRs and CNTs shown in Fig. 2. With disregard of the fine structure, the step spacing in conductance ladders of achiral graphene ribbons and carbon nanotubes are related as $\Delta_{\text{CNT}}^a = \Delta_{\text{CNT}}^z = 2\Delta_{\text{GR}}^a = 2\Delta_{\text{GR}}^z$, provided that the widths of armchair and zigzag ribbons (or the circumference lengths of respective nanotubes) is related as $N = \sqrt{3}N$. The minimal conductance of metallic

graphene ribbons equals G_0 . The minimal measured conductivity of graphene is about two times larger [9], that is equal to the initial value of the slope of conductance ladder of metallic graphene ribbons, see Fig. 2.

In summary, these results concern the problem that has been addressed in one way or another, in several dozens of publications. In part, they repeat previously reported findings: for example, the same conductance ladders we obtained for $(N,0)$ semiconducting carbon nanotubes can be inferred from the dispersion relations used by Mintmire and White for derivation of their "universal density of states" [13]. However, our corresponding results dispose the "nonuniversal" features of the CNT spectra, namely, the fine band structure of zigzag CNTs and blue shift of 1D bands of armchair CNTs. In many cases these play a crucial role. In previous works to the best of our knowledge, there is no comparable analytical description of graphene ribbons. The presented analysis strongly opposes the myth of "dispersionless mode" in the spectrum of graphene zigzag ribbons and discloses a number of weaknesses of relativistic speculations regarding electronic properties of honeycomb lattice structures.

* aleon@ifm.liu.se; We thank Linda Wylie for editing this manuscript. The work was partly supported by Special

Program of the Physics and Astronomy Section of NANU and by Visby program of the Swedish Institute.

- [1] B.J. van Wees, H. van Houten, C.W.J. Beenakker, J.G. Williamson, J.P. Kouwenhoven, D. van der Marel, and C.T. Foxon, *Phys. Rev. Lett.* **60** (1988) 848.
- [2] D.A. Wharam, T.J. Thornton, R. Newbury, M. Peper, H. Ahmed, J.E.F. Frost, D.G. Hasko, D.C. Piacock, D.A. Ritchie, and G.A.C. Jones, *J. Phys. C* **21** (1988) L209.
- [3] R. Landauer, *IBM J. Res. Dev.* **1** (1957); **32** (1988) 306.
- [4] M. Büttiker, *Phys. Rev. Lett.* **57** 1986 1761.
- [5] L.I. Glazman, G.B. Lesovick, D.E. Kmel'nitskii, and R.I. Shekhter, *Pis'ma Zh. Eksp. Teor. Fiz.* **48** (1988) 218 [*JETP Lett.* **48** 1988 238].
- [6] A. Szafer and A.D. Stone, *Phys. Rev. Lett.* **62** (1988) 300.
- [7] M. Büttiker, *Phys. Rev. B* **41** (1990) 7906.
- [8] L.I. Malysheva and A.I. Onipko, *J. Phys.: Cond. Matter* **7** (1995) 3597.
- [9] A.K. Geim and K.S. Novoselov, *Nature materials* **6** (2007) 183.
- [10] L. Malysheva and A. Onipko, arXiv:0801.4155v1 [cond-mat.mes-hall].
- [11] R.Saito, G. Dresselhaus, and M.S. Dresselhaus, *Physical Properties of Carbon Nanotubes* (imperial College, London, 1998).
- [12] S. Reich, C. Thomsen, and J. Maultzsch *Carbon Nanotubes: Basic concepts and Physical Properties* (WILEY-VCH, Weinheim, 2004).
- [13] J.W. Mintmire and C.T. White *Phys. Rev. Lett.* **81** (1998) 2506.
- [14] L. Malysheva and A. Onipko, arXiv:0802.1385v1 [cond-mat.mes-hall].